

The peak energy of dissipative GRB photospheres

Dimitrios Giannios[★]

Department of Astrophysical Sciences, Peyton Hall, Princeton University, Princeton, NJ 08544, USA

Received / Accepted

ABSTRACT

The radiation released at the transparency radius of an ultrarelativistic flow can account for the observed properties of gamma-ray bursts (GRBs) provided that sufficient energy is dissipated in the sub-photospheric region. Here, I investigate how the peak energy of the $Ef(E)$ spectrum and its overall shape depend on the properties of the jet for various “dissipative photospheres”. I find that continuous energy release which results in electron heating over a wide range of distances may be the key to explain the GRB emission. In this picture, the peak of the spectrum forms at a Thomson optical depth of several tens. The peak depends mainly on the bulk Lorentz factor Γ of the flow and can, therefore, be used to determine it. The Γ is predicted to range from ~ 10 to 1000 from X-ray flashes to the brightest observed GRBs in agreement with recent observational inferences. The Amati relation can be understood if the brightest bursts are the least baryon loaded ones. Implications from this interpretation of the GRB emission for the central engine are discussed.

Key words: Gamma rays: bursts – radiation mechanisms: general – methods: statistical

1 INTRODUCTION

Although several thousand gamma-ray bursts (GRBs) have been observed so far, the mechanisms responsible for the GRB emission remain elusive. Both synchrotron and photospheric models have been widely explored in the literature to explain the characteristic “Band-like” GRB spectrum which is characterized by smoothly connected power-laws (Band et al. 1993). The synchrotron models rely on a power-law electron distribution accelerated at large distance (or small optical depths) in the jet. The photospheric models focus, instead, on radiation that is released when the jet becomes transparent.

Photospheric models are attractive interpretation because they can result in high radiative efficiency and naturally predict peak energies $E_{\text{peak}} \sim 1$ MeV close to the observed values (Goodman 1986; Thompson 1994; Mészáros & Rees 2000). The value of E_{peak} in this interpretation is coupled to the main properties of the flow (e.g. luminosity L , and Lorentz factor Γ). Indeed, observations indicate that the peak of the $Ef(E)$ spectrum tracks the instantaneous gamma-ray luminosity and integrated energy during a burst and among different bursts, respectively (e.g., Amati et al. 2002; Yonetoku et al. 2004; Ghirlanda, Nava & Ghisellini 2010).

On the other hand, the energy dissipated in the base of the jet effectively thermalizes, so in the absence of additional dissipation at modest optical depths (i.e. further out) the emission from the transparency radius is quasi-thermal in sharp contrast to that typically observed. Significant dissipation of energy of some sort is required close to the photosphere of the flow to lead to the observed,

smoothly-connected power-law spectra. The source of such dissipation may be (strong or many, weak) shocks (Rees & Mészáros 1994; Lazzati & Begelman 2011), magnetic reconnection (Giannios 2006), or nuclear collisions (Beloborodov 2010).

Adopting the reconnection model for GRBs of Drenkhahn (2002), I have shown that magnetic dissipation leads to powerful photospheric emission (Giannios 2006). The observed \sim MeV peak of the spectrum forms at Thomson optical depth of several tens where radiation and electrons drop out of thermal equilibrium; the electrons turn hotter further out in the flow. Inverse Compton scattering at larger distance (smaller optical depth) leads to the high-energy tail that can extend well into the GeV range. A Band-like spectrum naturally forms in this scenario.

Here, I develop a generic dissipative photospheric model applicable to arbitrary dissipative process that results in electron heating. Both a flat rate of dissipation of energy (e.g. constant luminosity dissipated per decade of distance) and localized dissipation events are explored (Sections 2, 3). The model predicts a relation of the peak E_{peak} of the observed emission with the properties of the flow; most sensitively depending on the bulk Lorentz factor Γ (Section 4). Using the observed $E_{\text{peak}} - L_{\gamma}$ relation I make inferences for the central engine of GRBs (Section 4.1). Section 5 clarifies various aspects of the GRB variability in the context of the model. Discussion and conclusions are presented in Section 6.

2 DISSIPATIVE PHOTOSPHERES

Energy dissipated at the very inner parts of the jet flow quickly thermalizes. A substantial thermal component can also be built in an initially rather cold, magnetically dominated flow when magnetic

[★] E-mail: giannios@astro.princeton.edu

energy is dissipated at large Thomson optical depth $\tau \gg 1$, e.g. as expected in a striped wind model (Drenkhahn & Spruit 2002). The thermal luminosity L_{th} (dominated by radiation) is released at the transparency radius (defined as the distance at which $\tau = 1$). For typical parameters of the jet flow, the resulting quasi-thermal emission peaks at $E_{\text{peak}} \sim 3k_B T_{\text{obs}} \sim 0.1 - 1$ MeV (Goodman 1986, Thompson 1994; Daigne & Mochkovitch 2002; Beloborodov 2010), very close to the typically observed values (Band 1993). In the absence of dissipation of energy close to the photosphere, however, the emerging emission cannot account for the observed GRB spectrum. Though isolated cases for a strong quasi-thermal component in the GRB emission have been made (Ryde 2005; Ryde et al. 2010; Ryde et al. 2011), *the GRB spectrum generically has non-thermal appearance*.

The photospheric emission is, however, modified when additional energy release takes place close to the transparency radius. It turns out (see next Section) that continuous electron heating at a range of optical depths from $\tau \sim \text{several tens}$ out to ~ 0.1 may be the key to reproduce the observed emission. Continuous dissipation results in a well defined distance where radiation and particles drop out of equilibrium, the so-called *equilibrium radius*. The peak of the emission spectrum is determined by the plasma temperature at this distance. Below we develop a general framework to calculate the peak of the spectrum as function of the properties of the flow.

2.1 A generic model

Consider a jet coasting with bulk Lorentz factor Γ , total isotropic equivalent luminosity L and baryon loading $\eta \equiv L/\dot{M}c^2 \gtrsim \Gamma$. In the presence of energetic particles injected by the dissipative process, the flow can be loaded with a modest number of pairs (Pe'er et al. 2006; Vurm et al. 2011). Assuming f_{\pm} electron+positron pairs per proton (i.e. $f_{\pm} = 1$ for $e - p$ plasma; hereafter pairs are referred to as electrons¹), the rest-frame electron number density is $n_e = f_{\pm} L / 4\pi r^2 \eta \Gamma m_p c^3$. Clearly both Γ and f_{\pm} can vary with distance (because of acceleration of the flow and energetic particle injection that result in pair creation, respectively). Here, I treat these quantities as constants with the main focus been on their values close to the equilibrium radius. The Thomson optical depth $\tau \equiv n_e \sigma_T r / \Gamma$ as function of distance is

$$\tau = 37 \frac{L_{53} f_{\pm}}{r_{11} \eta_{2.5} \Gamma_{2.5}^2}, \quad (1)$$

where all quantities are in cgs units and the $A = A_x 10^x$ notation is adopted. Setting $\tau = 1$, the Thomson photosphere is located at

$$r_{\text{ph},11} = 37 \frac{L_{53} f_{\pm}}{\eta_{2.5} \Gamma_{2.5}^2}. \quad (2)$$

We consider a flow which carries a thermal component of luminosity L_{th} that is a substantial fraction ϵ of that of the flow: $L_{\text{th}} = (4/3)4\pi r^2 \Gamma^2 a T_{\text{th}}^4 c = \epsilon L$. This can be realized in both fireballs and dissipative, magnetically dominated flows (e.g. Drenkhahn 2002). The (rest frame) plasma temperature is

$$k_B T_{\text{th}} = 1.1 \frac{\epsilon^{1/4} L_{53}^{1/4}}{r_{11}^{1/2} \Gamma_{2.5}^{1/2}} \text{ keV}. \quad (3)$$

Inspection of eqs. (2) and (3) reveals that the plasma typically cools to sub-keV temperature close to the photosphere. It turns out, however, that the dissipative process heats up the flow to a temperature well in excess of T_{th} before it reaches the photosphere.

Suppose that a dissipative process injects energy in the flow heating the electrons (see Section 3 for discussion on the physical justification of such assumption). I consider two different situations for the radial dependence of the dissipation rate: i) a gradual rate of energy release of rather flat profile (i.e. constant rate of energy dissipated per e-folding of distance): $dL_{\text{d}}/dr = L_{\text{d},0}/r$ and ii) dissipation that is localized to a narrow range in distance.

In the case of the gradual energy release, the heating rate per unit volume in the rest frame of the flow is $P_{\text{h}} = L_{\text{d},0}/4\pi r^3$. If the thermal component L_{th} is built by the dissipation of energy from smaller distances (and including adiabatic cooling of the photons) one gets $L_{\text{th}} = (3/2)L_{\text{d},0}$. Allowing for a comparable amount of additional heating even deeper in the flow, we set $L_{\text{d},0} = L_{\text{th}}/3 = \epsilon L/3$.

Heating of the electrons is balanced by radiative cooling². Electrons and photons are in thermal equilibrium at large depth with their common temperature given by eq. (3)³. This equilibrium is broken once heating and cooling balance leads to $T_e > T_{\text{th}}$. It can be shown (see Giannios 2006) that Compton cooling $P_{\text{IC}} = 4n_e \Theta_e c \sigma_T U_r$ is the dominant cooling mechanism for the electrons in this region ($\Theta_e = k_B T_e / m_e c^2$ and U_r is the energy density of radiation). Equating dissipative heating and cooling ($P_{\text{h}} = P_{\text{IC}}$) and setting $U_r = a T_{\text{th}}^4$ one derives the electron temperature as function of distance

$$k_B T_e = 1.5 \frac{r_{11} \Gamma_{2.5}^2 \eta_{2.5}}{f_{\pm} L_{53}} \text{ keV}. \quad (4)$$

The location where radiation and electrons drop out of equilibrium is found by setting $T_{\text{th}} = T_e$, defining the (maximum) *equilibrium radius* r_{eq} :

$$r_{\text{eq},11} = 0.80 \frac{L_{53}^{5/6} \epsilon^{1/6} f_{\pm}^{2/3}}{\Gamma_{2.5}^{5/3} \eta_{2.5}^{2/3}}. \quad (5)$$

At the equilibrium radius r_{eq} , the Thomson optical depth and the temperature of the electrons are, respectively

$$\tau_{\text{eq}} = 46 \frac{L_{53}^{1/6} f_{\pm}^{1/3}}{\epsilon^{1/6} \Gamma_{2.5}^{1/3} \eta_{2.5}^{1/3}} \quad (6)$$

and

$$k_B T_{\text{eq}} = 1.2 \frac{\epsilon^{1/6} \Gamma_{2.5}^{1/3} \eta_{2.5}^{1/3}}{L_{53}^{1/6} f_{\pm}^{1/3}} \text{ keV}. \quad (7)$$

Note that the optical depth and temperature of the plasma at the equilibrium radius depend very weakly on the flow parameters and are in the range of several tens and ~ 1 keV, respectively. The equilibrium radius is of particular importance since it is the location at which the peak of the spectrum forms under a wide range of conditions. The observed peak of the spectrum is

$$E_{\text{peak}} \simeq \frac{4}{3} 3\Gamma k_B T_{\text{eq}} \simeq 1.5 \frac{\epsilon^{1/6} \Gamma_{2.5}^{4/3} \eta_{2.5}^{1/3}}{L_{53}^{1/6} f_{\pm}^{1/3}} \text{ MeV}. \quad (8)$$

² Adiabatic cooling can be shown to be negligible for the electrons.

³ In reality, the electrons maintain a slightly higher temperature from radiation because of external heating.

¹ For a photospheric GRB model where the flow does not contain baryons see Ioka et al. (2011).

At distance $r > r_{\text{eq}}$, and using eqs. (1) and (4), the Compton y parameter⁴ is found to be $y = 4\Theta_e \tau \sim 0.4$ independently of distance or the parameters of the flow leading to significant up-scattering of the photons. The Compton parameter is close to unity because the incoming radiative luminosity L_{th} and dissipation rate $L_{\text{d,o}}$ are comparable. Up-scattering of the radiation emerging from r_{eq} at larger distance leads to broader spectra and to a flat high-energy tail above E_{peak} . The high-energy tail is followed by an exponential cutoff at the energy that corresponds to the electron temperature at the distance where the dissipation stops (see next section).

2.2 Numerical Results

The analytical arguments presented in the previous Section are fully supported by detailed Monte-Carlo radiative transfer simulations. The code developed in Giannios (2006) is used to study the electro-magnetic spectrum emerging from a dissipative photosphere. The inner boundary of the calculation is set at the equilibrium radius where photons following a thermal distribution of temperature T_{eq} are injected. The photons are followed throughout the photosphere until the flow reaches an optical depth of $\tau = 0.1$ where the outer boundary is set. The calculation includes Compton scattering, relativistic effects, while the electron temperature is iterated until the heating rate is matched by Compton cooling everywhere in the flow. We do not include synchrotron emission and non-thermal particle acceleration. While both are important in determining the exact spectrum, they are model dependent. For this paper, however, it is important that the peak of the emission is set at the distance where radiation and matter drop out of equilibrium and rather independently of the details of non-thermal processes. In the following, both extended dissipation with $dL_{\text{d}}/dr = L_{\text{d,o}}/r$ and localized dissipation are investigated.

2.2.1 Extended Dissipation

Assuming extended dissipation of energy, in Fig. 1 I plot the radiation spectrum at various distances of the flow for the reference values of the parameters ($L = 10^{53} \text{ erg}\cdot\text{s}^{-1}$, $\eta = \Gamma = 300$, $\epsilon = 0.3$, $f_{\pm} = 1$). Note that the thermal emission at r_{eq} evolves into one of non-thermal appearance when passing through the $\tau = 1$ surface building a flat high-energy tail. Inverse Compton scattering with Compton y parameter $y \lesssim 1$ results in a flat ($Ef(E) \sim E^0$) emission above the peak. The outer boundary of the calculation is set at larger distance that corresponds to $\tau = 0.1$. The high-energy cutoff E_{cut} is determined by the temperature of the electrons at the outer boundary (in this example $k_B T_{\text{e,out}} \simeq 300 \text{ keV}$ resulting in $E_{\text{cut}} \simeq \Gamma k_B T_{\text{e,out}} \simeq 100 \text{ MeV}$). While in this paper, I set the outer boundary of dissipation by hand at $\tau = 0.1$, more detailed models, such as the magnetic reconnection model of Drenkhahn & Spruit (2002) predict where this cutoff takes place.

In Fig. 2 I show the resulting spectra for different values of the parameters. The peak of the emission E_{peak} is very close to the analytic expression (8). The overall shape of the spectra is very similar with only the peak and cutoff energies depending on the parameters. A Band-like spectrum is reproduced for very different parameters of the flow. The high-energy tail has spectral slope $f(E) \propto E^{\beta}$ with $\beta \lesssim -1$ as observed. Below the peak energy the slope, as measured in the 10-100 keV range, is $f(E) \propto E^{\alpha}$ with $\alpha \sim 0 - 1$.

⁴ For relativistically expanding fluid the number of scatterings scales as $\sim \tau$ and not $\propto \tau^2$ as in a static medium (see Giannios 2006).

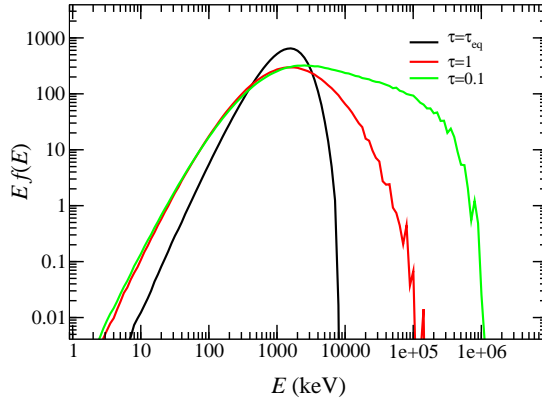


Figure 1. Numerically calculated spectra at different optical depths in the jet for the reference values of the parameters and for extended dissipation of energy. The thermal injected photon spectrum at the equilibrium radius (black line) evolves into a broader spectrum at the $\tau = 1$ surface (red line) and develops a flat power-law tail at the outer radius (corresponding to $\tau = 0.1$; green line). The peak of the $Ef(E)$ emerging spectrum is determined at the equilibrium radius.

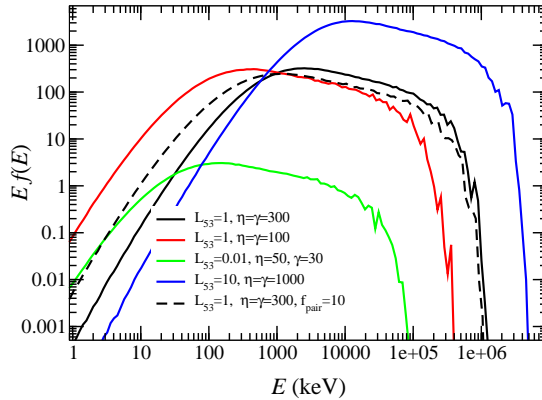


Figure 2. Emerging spectra for different values of the parameters and for extended dissipation of energy. The spectrum has a Band-like shape practically independently of the luminosity, baryon loading and Lorentz factor of the flow. The peak of the spectrum follows the scaling predicted by eq. (8). The high energy cutoff is set by the location of the outer boundary of the simulation.

The slope α is consistent but in the rather hard range in comparison with the observed distribution. Note, however, that synchrotron and synchrotron-self-Compton emission from larger distances (not included in this work) can soften the spectrum below the peak (Giannios 2008; Uhm, Beloborodov & Poutanen 2011).

2.2.2 Localized Dissipation

The process that dissipates energy in the jet may result in energy release over a narrow range of distances. Here, I investigate how a thermal component carried by the flow is modified depending on the optical depth at which such energy release takes place.

I assume that the thermal component $L_{\text{th}} = \epsilon L$ is reprocessed

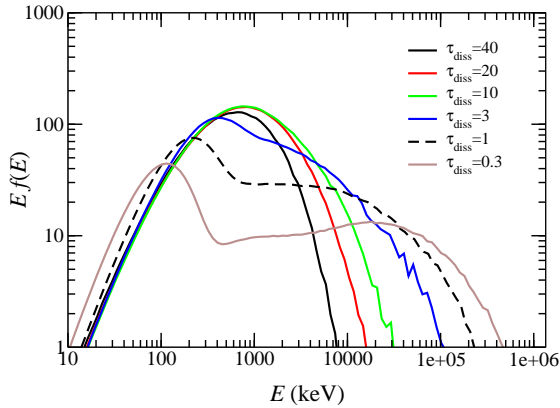


Figure 3. Emerging spectrum for dissipation of energy at a narrow range of distance (or optical depth τ_{diss}) for different τ_{diss} . Dissipation at large optical depths $\tau_{\text{diss}} \gtrsim 10$ leads to narrow emission spectrum. Dissipation at $\tau_{\text{diss}} \lesssim 1$ leads to distinct thermal and high-energy components. For $\tau_{\text{diss}} \sim 3$ the two components are smoothly connected.

by Compton up-scattering through a narrow region of hot electrons. The electrons are heated at a rate $L_{\text{d},0} = L_{\text{th}}$ over a range of Thomson depth $\tau_{\text{diss}} \dots \tau_{\text{diss}}/2$ (i.e. a factor 2 in distance). The electron temperature is determined by heating-cooling balance. Setting the various parameters to their reference values, Fig. 3 shows the emerging spectrum for different values of τ_{diss} . Dissipation at large optical depths $\tau_{\text{diss}} \gtrsim 10$ leads to a broadened, Planck-like distribution. The resulting narrow emission spectrum has a steep rise/decline below/above the peak. Dissipation at $\tau_{\text{diss}} \lesssim 1$ leads to a hot region above the photosphere. Most of the photons do not interact with the hot electrons leading to a distinct quasi-thermal component while; photons that are up-scattered at least once form a high-energy component. Although occasionally GRB spectra show such multi-component behavior in the keV-MeV regime, this is not typical. For $\tau_{\text{diss}} \sim 3$ the two components are smoothly connected and the resulting spectrum compares more favorable with observations. For a model where the dissipation (through magnetic reconnection) takes place at a narrow region of $\tau \gtrsim 1$ see Thompson (1994).

Summarizing, localized dissipation in general does not account for observations because it either leads to narrow or multi-component spectra in the \sim MeV energy range. There is a limited range of optical depths of $\tau_{\text{diss}} \sim 3 - 5$ where dissipation results in a smooth Band-like spectrum.

3 THE DISSIPATIVE MECHANISMS

In the previous analysis we simplified the calculation assuming thermal electrons continuously heated by an external agent. Here we elaborate on the possible sources for smooth “volume” heating of the GRB flow (Ghisellini & Celotti 1999; Stern & Poutanen 2004; Pe’er, Mészáros & Rees 2006).

Models for gradual energy release that heats the electrons involve magnetic reconnection (Giannios 2006), multiple weak shocks (Ioka et al. 2007; Lazzati & Begelman 2010)⁵ and neutron-

proton collisions (Beloborodov 2010). In the first case, the energy is initially stored in the magnetic field while in the latter cases in relative bulk motions within the jet. In the following I argue that, independently of the dissipative mechanism, a large fraction of the energy dissipated close to the equilibrium radius is expected to be stored to (mildly) relativistic protons. Coulomb $e - p$ collisions effectively drive the energy from protons into the electrons (see Beloborodov 2010). The electrons then transfer their energy into the photon field through Compton scattering. The characteristic electron equilibrium temperature is sub-relativistic and determined by heating-cooling balance.

Multiple weak shocks in the jet or elastic neutron-proton collisions (close to the distance where the neutron and proton fluids decouple) can be expected to heat the protons at mildly relativistic temperatures with the heating maintained over a range of distances in the jet. When the heating takes place at optical depth of tens, the Coulomb coupling of \lesssim GeV protons with \sim keV electrons (see, e.g., Stepney 1983) can be shown to be effective in transferring the energy into the electrons within one expansion timescale of the jet. These, slowly heated, electrons pass their energy into the photon field effectively through inverse Compton scattering. In addition to mildly relativistic protons, shocks and inelastic $n - p$ collisions can inject high-energy particles. Non-thermal processes can result in a modest pair loading in the jet (Pe’er et al. 2006; Beloborodov 2010)⁶ but not expected to directly affect the peak energy of the emission as long they are not energetically dominant.

Magnetic reconnection can take place effectively at large optical depths (deep in the jet) through, e.g., tearing instabilities of the current sheet (Loureiro, Schekochihin & Cowley 2007; Uzdensky, Loureiro & Schekochihin 2010) assisted/induced by the acceleration of the jet (Lyubarsky 2011).⁷ Magnetic reconnection takes place in multiple dissipative centers that accelerate particles, heat the plasma and drive fast bulk motions. The fast motions in the downstream of the reconnection region are required for sufficiently fast reconnection. The bulk motions are dissipated further downstream in shocks resulting in hot protons. Coulomb collisions can effectively couple the proton energy to the electrons which, in turn, couple it to the radiation field (as discussed above). In this strongly magnetized plasma ($U_B \gtrsim U_{\text{ph}}$), sub-relativistic electrons can thermalize very efficiently through exchange of synchrotron photons (the so-called “synchrotron boiler”; Ghisellini et al. 1998) before they have the chance to cool through inverse Compton scattering. An alternative picture where the energy released in the reconnection process drives MHD waves (instead of bulk motions) is described in Thompson (1994). Photons extract the energy from the waves through scattering on electrons (Compton drag). Also in this picture the electron velocity is limited to sub-relativistic speed and close to a Compton equilibrium with the radiation field. The analysis of the previous section may apply to this scenario as well.

In summary the details of the dissipation process (and the related non-thermal processes) may well affect the pair injection rate and result in additional features in the spectrum (e.g. powering a pair annihilation line at $E \sim \Gamma m_e c^2$) but do not change the basic

taneously to ultrarelativistic energies leaving them to cool radiatively on a longer time scale (see, however, Ramirez-Ruiz 2005).

⁶ Note, however, that if the energy density of the magnetic field is higher than that of the radiation, ultrarelativistic electrons cool mainly through synchrotron emission and the pair creation is further limited.

⁷ A possible speed up of the reconnection rate at Thomson thin conditions (Lyutikov & Blandford 2003; McKinney & Uzdensky 2012) can have interesting implications but is not required in this picture.

⁵ The, more often invoked for the GRB emission, strong internal shocks (Rees & Mészáros 1994) are unlikely to lead to smooth/gradual heating of the electrons. Such shocks, instead, accelerate particles practically instan-

picture of sub-relativistic electrons strongly coupled to the radiation field with their energy determined by a balance of dissipative heating and radiative cooling. It is this basic process at the equilibrium radius that determines the peak of the emerging emission.

4 INFERRING THE BULK LORENTZ FACTOR OF THE FLOW

In this rather general framework of dissipative photospheres, there is a close connection between the peak of the spectrum and the properties of the flow summarized in eq. (8). Eq. (8) can be solved in terms of Γ :

$$\Gamma = 280 E_{\text{peak, MeV}}^{3/5} \epsilon_{-0.5}^{-1/10} L_{53}^{1/10} f_{\pm}^{1/5} \left(\frac{\eta}{\Gamma} \right)^{-1/5}, \quad (9)$$

where I chose to express Γ as function of the ratio $\eta/\Gamma \gtrsim 1$ instead of η . A clear implication from the last expression is that Γ depends mainly on the peak energy E_{peak} with extremely weak dependence on the physical properties of the jet. To first approximation, one can have a fair estimate of the Lorentz factor just from the observed peak of the GRB emission. From eq. (9) it is clear that the model predicts that the high-peaked GRBs come from faster jets. This is in sharp contrast to the synchrotron internal shock model where the opposite holds true ($E_{\text{peak}} \propto \Gamma^{-2}$).

One can somewhat improve on the estimate of the bulk Γ of the jet from observables by assuming a gamma-ray luminosity $L_{\gamma} \sim \epsilon L$ and using the observed L_{γ} and $\epsilon \sim 1$. This interpretation of the peak of the emission implies that the brightest GRBs with $E_{\text{peak}} \sim$ several MeV and $L_{53} \sim 10$ (e.g. Abdo et al. 2009) come from the most relativistic $\Gamma \sim 1000$ flows while weaker X-ray flashes with $E_{\text{peak}} \sim 30$ keV and $L_{53} \sim 0.01$ come from “slower” jets of $\Gamma \sim 20$. Low-luminosity GRBs (e.g. Soderberg et al. 2006) and the X-ray flares that follow many bursts (Burrows et al. 2005; Chincarini et al. 2010) can also be a result of a dissipative photosphere from yet slower jets of $\Gamma \lesssim 10$. In particular low-luminosity GRBs may come from $\Gamma \sim 3$ jets that result in only modest relativistic beaming of their emission and may, therefore, account for the larger observed local rate of these events (Soderberg et al. 2006) in comparison to classical GRBs. As discussed in Section 6, observational estimates of the Lorentz factor of GRBs support the model prediction that higher E_{peak} bursts are coming from higher Γ flows.

4.1 Additional inferences for the flow using observed correlations of the GRB emission

It has been recognized for some time that various *time integrated* quantities over the duration of a burst may correlate with each other, e.g., the peak energy E_{peak} with the isotropic gamma-ray energy E_{γ} (Amati et al. 2002). Even in the presence of outliers (Band & Preece 2005; Nakar & Piran 2005), these correlations may teach us a lot about the GRB physics. The emission in the photospheric models is, however, connected to the *instantaneous* properties of the flow. A change in any of the properties (e.g. luminosity or baryon loading) during the burst shifts the location of the photosphere and its appearance. Ghirlanda et al. (2010; 2011) found that there is a time dependent Amati-like relation of $E_{\text{peak}}(t)$ and $L_{\gamma}(t)$ during the evolution of bursts where $E_{\text{peak}} \simeq 1 L_{\gamma, 53}^{1/2}$ MeV.

If this relation is verified by more data, it implies for the photospheric models that the Lorentz factor correlates with the luminosity of the flow. In this interpretation, one can derive an estimate

of the Lorentz factor of the flow directly from the observed gamma-ray luminosity using eq. (9), the instantaneous $E_{\text{peak}} - L_{\gamma}$ correlation and that $L_{\gamma} \sim L_{\text{th}} = \epsilon L$:

$$\Gamma = 310 E_{\text{peak, MeV}}^{4/5} \epsilon_{-0.5}^{-1/5} f_{\pm}^{1/5} \left(\frac{\eta}{\Gamma} \right)^{-1/5}. \quad (10)$$

Note that the Lorentz factor depends sensitively on a single observable, namely, the peak energy. Therefore, E_{peak} can be used to infer the Lorentz factor. In terms of properties of the flow, I find that $\Gamma = 200 \epsilon_{-0.5}^{1/5} L_{53}^{2/5} (\eta/\Gamma)^{-1/5} f_{\pm}^{1/5}$, i.e., that more luminous bursts are less baryon loaded with $\Gamma \propto L^{2/5}$. Note, however, that a systematic dependence of any other quantity with, say, the luminosity of the flow can distort this $\Gamma - L$ scaling. Finally, the $\Gamma - L$ relation can be combined with eq. (7) to find the temperature of the flow at the equilibrium radius:

$$k_B T_{\text{eq}} \simeq 0.8 \epsilon_{-0.5}^{3/10} L_{53}^{1/10} f_{\pm}^{-1/5} \left(\frac{\eta}{\Gamma} \right)^{1/5} \text{ keV}. \quad (11)$$

Note that the temperature of the flow clusters in the \sim keV range and has very weak dependence on the parameters of the jet. As discussed in Section 6 such clustering of the peak of the emission in the rest frame of the flow has been observed.

The instantaneous $E_{\text{peak}} - L_{\gamma}$ relation also puts interesting constraints on the distance where the peak of the spectrum forms. Using the expression (5) for r_{eq} and eq. (10), I arrive to

$$r_{\text{eq}} = 2.1 \times 10^{11} L_{53}^{-1/10} \epsilon_{-0.5}^{-3/10} f_{\pm}^{1/5} \left(\frac{\eta}{\Gamma} \right)^{-1/5} \text{ cm}. \quad (12)$$

The equilibrium distance r_{eq} depends very weakly on the various parameters. Even allowing for orders of magnitude variations in the luminosity and (as expected) more modest changes in other parameters from burst to burst (or during the evolution of a burst), r_{eq} varies at most by a factor of a few.

5 GRB VARIABILITY

GRBs are variable on timescales as short as milliseconds. Their lightcurves are characterized by multiple pulses (e.g. Fenimore et al. 1995) that typically last for seconds and show characteristic spectrum that often evolves from hard to soft (e.g. Hakkila & Preece 2011) and/or tracks the instantaneous flux of the flow (e.g. Ghirlanda et al. 2011). Can the photospheric model account for the temporal GRB behaviour?

The small radius of emission in the photospheric models allows for fast variability down to $t_v \sim r_{\text{ph}}/2\Gamma^2 c \sim$ sub-msec timescales (depending on the parameters of the flow; see also Gianfranceschi & Spruit 2007). Allowing the continuous heating out to optical depth $\tau \sim 0.1$ ($r_{\text{out}} = 10 r_{\text{ph}}$) can lead to the multi MeV high-energy tail delayed by $r_{\text{out}}/2\Gamma^2 c \sim$ several msec with respect to the MeV peak (with the GeV emission potentially more delayed depending on the distance at which it takes place). The steady-state jet model developed here is not applicable to study extremely short (sub-msec) timescales (for which the steady-state assumption breaks down) but is well suited to study the evolution of the burst on longer timescales. In particular, the \sim sec duration GRB pulses can be accurately studied as a sequence of steady state models where the properties of the jet ($L = L(t)$, $\Gamma = \Gamma(t)$, etc) vary on this timescale. The observed variability on second timescales in the well studied $\sim 10 - 1000$ keV energy range is likely to be dominated by temporal evolution of the properties of the jet rather than delays introduced by propagation effects of the ejecta.

The spectral evolution during a GRB pulse depends on how

$\Gamma(t)$ and $L(t)$ evolve during the pulse. Giannios & Spruit (2007) have shown that If , for instance, $\Gamma(t)$ has a positive power-law dependence on $L(t)$ during individual pulses then the peak of the spectrum tracks the observed flux (as seen observationally in Ghirlanda et al. 2011). In this case, while the flux declines after the peak luminosity of a pulse, the peak of the emission spectrum also declines and the spectrum softens. As a result the pulse duration on the softer X-ray bands is longer than in the harder ones.

In summary, continuous dissipation close to the photosphere can allow for fast evolving (sub-msec) emission. Furthermore, it is possible to account for observed temporal properties of GRBs given specific assumptions about the behaviour of the central engine. The reasons for which the engine operates in such a fashion is, however, not addressed by this work.

6 DISCUSSION AND CONCLUSIONS

In this paper, I have explored a wide range of “dissipative photosphere” models to pin down the location where the peak E_{peak} of the spectrum forms and how it connects to the properties of the jet. The resulting expression (9) of my analysis summarizes this connection, is quite general and rather independent of the physical model for energy dissipation.

I have explored both localized and continuous in distance dissipation of energy. Localized heating of electrons over a narrow range of distance is shown here to have difficulties to account for observations. If the dissipation takes place at large optical depth, the emerging spectrum is rather narrow, while dissipation at $\tau \lesssim 1$ has two distinct components in the \sim MeV energy range, both in conflict to the majority of observed bursts. However, localized dissipation that takes place at optical depth $\tau \sim 3$ results in a more promising spectrum. Thompson (1994) discusses a scenario where such dissipation is possible.

I find that *continuous* dissipation of energy over a wide range of optical depths can naturally give the Band-like spectrum with peak and slopes above and below the peak at the observed range. Magnetic reconnection in a jet that contains small-scale field reversals naturally results in such flat dissipation profile throughout the photospheric region. Alternatives such as multiple, weak shocks or neutron-proton collisions can also result in continuous energy injection. The MeV peak of the spectrum forms at the distance where radiation and the electrons drop out of thermal equilibrium. In the context of this model the peak energy is mainly determined by the bulk Lorentz factor of the flow. The observed E_{peak} can, therefore, be used to infer Γ .

The model predicts that the peak energy E_{peak} positively correlates with Γ . I find that weak GRBs (the spectrum of which peaks in the X-ray regime; the so called X-ray flashes) and X-ray flares that follow the bursts potentially come from $\Gamma \sim 10$ jets while the brightest observed *Fermi-LAT* bursts, with peak energy at several MeV, come from the fastest $\Gamma \sim 1000$ flows. Recently (Ghirlanda et al. 2012) used the peak time of the afterglow emission to estimate the bulk Lorentz factor Γ of 31 GRBs. They verified that brighter bursts are characterized by higher Γ and showed that the peak energy of the emission at the rest frame of the jet clusters at several keV; both findings are unique predictions of this work (see eqs. 7, 11).

The observed relation of the peak of the spectrum with the *instantaneous* burst luminosity indicates a close coupling of the emerging spectrum to instantaneous properties of the flow (Ghirlanda et al. 2011). It has already been pointed out in Gian-

nios & Spruit (2007) that the $E_{\text{peak}} - L_\gamma$ relation implies, in the context of the reconnection model, that brighter segments of a burst come from higher Γ (i.e., “the brighter the cleaner”) jet. I come to the same conclusion for the generic photospheric model developed here where the bulk Lorentz factor Γ and the luminosity of the flow L scale as, roughly, $\Gamma \propto L^{2/5}$. Note again that independent constraints coming from afterglow modeling indicate a similar correlation for Γ and the gamma-ray energy E_γ (Liang et al. 2010).

In this model, the MeV peak forms in a fairly compact region, while the high-energy tail forms at a larger distance. The tail can extend to multi-GeV energy without suffering attenuation due to pair creation and can exhibit delays of the order of $r_{\text{GeV}}/\Gamma^2 c$ with respect to the MeV emission that may be of order of seconds (as observed in some *Fermi-LAT* bursts, see Abdo et al. 2009; r_{GeV} is the radius where GeV emission takes place). While a different mechanism may be invoked for the dissipation at large distance that leads to the GeV emission (Mészáros & Rees 2011), the continuous spectrum from MeV to GeV energy indicates a single dissipative mechanism⁸ (see, e.g., Bosnjak & Kumar 2012).

Interestingly, using the observed instantaneous $E_{\text{peak}} - L_\gamma$ relation, the equilibrium distance r_{eq} (where the peak of the emission is set) can be shown to depend extremely weakly on the parameters of the flow with $r_{\text{eq}} \simeq 2 \times 10^{11}$ cm. This value is similar to the radii of Wolf-Rayet stars, probable progenitors of long-duration GRBs. This could indicate that interactions of the jet with the progenitor are important for energy dissipation (e.g. Lazzati & Begelman 2010). On the other hand, a similar correlation is observed in short-duration GRBs, supporting the idea of a progenitor-independent dissipative mechanism (Ghirlanda et al. 2011).

The inferred “the brighter the cleaner” property of GRB flows has profound implications for the nature of the central engine. Both accreting black holes and rapidly rotating magnetars have been invoked for launching the jet. Models that invoke accretion into a black hole (Woosley 1993) are not sufficiently developed to predict the amount of baryons that make it into the jet. In the millisecond magnetar model for GRBs (Usov 1992; Metzger et al. 2011), the calculation of the baryon loading is more tractable. The magnetars born with the strongest fields drive the brightest bursts and also give, averaged over the GRB duration, less baryon loaded flows. In particular, oblique rotators result in $\Gamma \propto L^{0.6}$ (but with a large scatter; see Metzger et al. 2011). This is a rather intriguing result since it might point to a rather complete picture for GRB physics (which is, however, hardly unique). A central engine consists of a proto-magnetar (with its magnetic field axis, in general, misaligned to the rotational axis), that gives rise to a magnetically dominated jet that contains field reversals on small scale (striped wind). Magnetic reconnection proceeds in the jet at a wide range of distances from the central engine and at a rather flat rate (Drenkhahn & Spruit 2002). The bright MeV emission of the GRB emerges from the Thomson photosphere of the flow while residual dissipation can extend the high-energy tail above the MeV peak well into the GeV regime (Giannios 2008).

ACKNOWLEDGMENTS

DG acknowledges support from the Lyman Spitzer, Jr. Fellowship awarded by the Department of Astrophysical Sciences at Princeton University and from the Fermi 4 Cycle grant number 041305.

⁸ but not necessarily a single emitting region for the MeV and GeV emission.

REFERENCES

- Abdo A. A., Ackermann M., Arimoto M. et al., 2009, *Science*, 323, 1688
- Amati L., Frontera F., Tavani M. et al., 2002, *A&A*, 390, 81
- Band D., Matteson J., Ford L. et al., 1993, *ApJ*, 413, 281
- Band D. L., Preece R. D., 2005, *ApJ*, 627, 319
- Beloborodov A. M., 2010, *MNRAS*, 407, 1033
- Bosnjak Z., Kumar, P., 2012, *MNRAS*, 421, L39
- Burrows D. N., Romano P., Falcone A. et al., 2005, *Science*, 309, 1833
- Chincarini G., Mao J., Margutti R. et al., 2010, *MNRAS*, 406, 2113
- Daigne F., Mochkovitch R., 2002, *MNRAS*, 336, 1271
- Drenkhahn G., 2002, *A&A*, 387, 714
- Drenkhahn G., Spruit H. C., 2002, *A&A*, 391, 1141
- Fenimore E. E., in 't Zand J. J. M., Norris J. P., Bonnell J. T., Nemiroff R. J., 1995, *ApJ*, 448, L101
- Ghirlanda G., Nava L., Ghisellini G., 2010, *A&A*, 511, A43
- Ghirlanda G., Ghisellini G., Nava L., 2011, *MNRAS*, 418, L109
- Ghirlanda G., Nava L., Ghisellini G. et al., 2012, *MNRAS*, 420, 483
- Ghisellini G., Haardt F., Svensson R., 1998, *MNRAS*, 297, 348
- Ghisellini G., Celotti A., 1999, *A&AS*, 138, 527
- Giannios D., 2006, *A&A*, 457, 763
- Giannios D., 2008, *A&A*, 480, 305
- Giannios D., & Spruit H. C., 2007, *A&A*, 469, 1
- Goodman J. 1986, *ApJ*, 308, L47
- Hakkila J., Preece R. D., 2011, *ApJ*, 740, 104
- Ioka K., Murase K., Toma K., Nagataki S., Nakamura T., 2007, *ApJ*, 670, L77
- Ioka K., Ohira Y., Kawanaka N., Mizuta A., 2011, *Progress of Theoretical Physics*, 126, 555
- Liang E.-W., Yi S.-X., Zhang J. et al., 2010, *ApJ*, 725, 2209
- Lazzati D., Begelman M. C., 2010, *ApJ*, 725, 1137
- Loureiro N. F., Schekochihin A. A., Cowley S. C., 2007, *Physics of Plasmas*, 14, 100703
- Lyubarsky Y., 2010, *ApJ*, 725, L234
- Lyutikov M., Blandford R., 2003, *ArXiv e-prints*, arXiv:astro-ph/0312347
- McKinney J. C., Uzdensky D. A., 2012, *MNRAS*, 419, 573
- Mészáros P., Rees M. J., 2000, *ApJ*, 530, 292
- Mészáros P., Rees M. J., 2011, *ApJ*, 733, L40
- Metzger B. D., Giannios D., Thompson T. A., Bucciantini N., Quataert E., 2011, *MNRAS*, 413, 2031
- Nakar E., Piran T., 2005, *MNRAS*, 360, L73
- Pe'er A., Mészáros P., Rees M. J., 2006, *ApJ*, 642, 995
- Ramirez-Ruiz E., 2005, *MNRAS*, 363, L61
- Rees M. J., Mészáros P., 1994, *ApJ*, 430, L93
- Ryde F., 2005, *ApJ*, 625, L95
- Ryde F., Axelsson M., Zhang B. B. et al., 2010, *ApJ*, 709, L172
- Ryde F., Pe'er A., Nymark, T. et al., 2011, *MNRAS*, 415, 3693
- Soderberg A. M., Kulkarni S. R., Nakar E. et al., 2006, *Nat.*, 442, 1014
- Stepney S., 1983, *MNRAS*, 202, 467
- Stern B. E., Poutanen J., 2004, *MNRAS*, 352, L35
- Thompson C., 1994, *MNRAS*, 270, 480
- Usov V. V., 1992, *Nat.*, 357, 472
- Uzdensky D. A., Loureiro N. F., Schekochihin A. A., 2010, *Phys. Rev. Letters*, 105, 235002
- Vurm I., Beloborodov A. M., Poutanen J., 2011, *ApJ*, 738, 77
- Woosley S. E., 1993, *ApJ*, 405, 273
- Yonetoku D., Murakami T., Nakamura T. et al., 2004, *ApJ*, 609, 935